Spatio-temporal modeling of high-throughput multi-spectral images improves agronomic trait genomic prediction in hybrid maize

Nicolas Morales[a], Michael A. Gore[a], Lukas A. Mueller[a,b], Kelly R. Robbins[a]
[a]Plant Breeding and Genetics Section, School of Integrative Plant Science, Cornell University, Ithaca, NY, USA, 14853; [b]Boyce Thompson Institute, Ithaca, NY, USA, 14853

ABSTRACT

To accelerate plant breeding genetic gain, spatial heterogeneity must be considered. Previously, design randomizations and spatial corrections have increased understanding of genotypic, spatial, and residual effects in field experiments. This study proposes a two-stage approach for improving agronomic trait genomic prediction (GP) using high-throughput phenotyping (HTP) via unoccupied aerial vehicle (UAV) imagery. The normalized difference vegetation index (NDVI) is measured using a multi-spectral MicaSense camera and ImageBreed. The first stage separates additive genetic effects from local environmental effects (LEE) present in the NDVI throughout the growing season. Considered NDVI LEE (NLEE) are spatial effects from univariate/multivariate two-dimensional splines (2DSpl) and separable autoregressive (AR1) models, as well as permanent environment (PE) effects from random regression models (RR). The second stage leverages the NLEE within genomic best linear unbiased prediction (GBLUP) in two distinct implementations, either modelling an empirical plot-to-plot covariance (L) for random effects or modelling fixed effects (FE). Testing on Genomes-to-Fields (G2F) hybrid maize (*Zea mays*) field experiments in 2017, 2019, and 2020 for grain yield (GY), grain moisture (GM), and ear height (EH) improves heritability and model fit equally-or-greater than spatial corrections; however, genotypic effect estimation across replicates is not significantly improved. Electrical conductance (EC), elevation, and curvature from a 2019 soil survey significantly improve GP model fit, but less than NLEE. Soil EC and curvature are most correlated to univariate 2DSpl NLEE. Defining L significantly improves genomic heritability and model fit more than setting FE, and RR NLEE can most significantly improve GP for GY and GM.

Keywords: High-throughput phenotyping (HTP), multi-spectral imagery, genomic prediction (GP), spatial corrections, random regression model, soil electrical conductance (EC), soil curvature

1. INTRODUCTION

The importance of controlling for environmental heterogeneity in agricultural field experiments is well known[1,2,3,4]. In plant breeding where soil composition, elevation, slope, curvature, water content, and management can vary within field experiments, the genotypic effects driving important agronomic traits become confounded with the local environment. Design randomization can help control spatial variation to a large degree[5,6]; however, advanced statistical approaches, such as the separable autoregressive and two-dimensional spline models, can capture local dependence effects between experimental plots[7,8,9]. Aerial imaging can reliably measure high-throughput phenotypes (HTP) across the growing season for all experiment plots in the field, using unoccupied aerial vehicles (UAV) and other systems[10,11,12,13]. A widely studied class of HTP are vegetation indices (VI), particularly the normalized difference vegetation index (NDVI)[14,15]. VI HTP have successfully measured chlorophyll content, canopy extent, biomass, and water use efficiency among other applications[16,17,18,19]. Though alternative HTP from images exist, this study will focus on NDVI as a means to understand local environmental effects (LEE) in the field[20,21,22].

Applying whole-genome marker data for genomic prediction (GP) enables shorter breeding cycles[23]. Genomic best linear unbiased prediction (GBLUP) can predict traits in animals and plants, including

maize and wheat[24,25]. Furthermore, HTP VI can improve GP through multivariate approaches by leveraging genetic correlations as demonstrated for grain yield in wheat and biomass in soybean[26,27]. Recent studies have successfully proposed two-stage approaches and frameworks for incorporating HTP, such as detecting spatial effects using the SpATS package in the first stage and then creating P-spline hierarchical growth models in the second stage[28,29]. Building on previous work, this study proposes a two-stage approach for improving GP. The first stage separates NDVI LEE (NLEE) from additive genetic effects temporally, using either spatial corrections or random regressions. The second stage summarizes the NLEE within GBLUP using two distinct implementations, either modelling an empirical plot-to-plot covariance of random effects (L) or modelling fixed effects (FE).

2. MATERIALS AND METHODS

As part of the Genomes to Fields (G2F) program, inbred and hybrid maize field evaluations were planted at the Musgrave Research Station (MRS) in Aurora, NY[30]. Of importance to this study are the hybrid maize experiments planted in 2017, 2019, and 2020, named 2017_NYH2, 2019_NYH2, and 2020_NYH2, respectively. In all field experiments, the following agronomic traits were measured: grain yield (GY) (bu/acre), grain moisture (GM) (%), and ear height (EH) (cm). Genotyping-by-sequencing (GBS) resulted in 945,574 single nucleotide polymorphisms (SNPs) across the genome for 1577 samples representing a total of 1325 unique maize inbred lines[31]. Genotypes were filtered for SNPs with minor allele frequency <5% or with >40% missing data, and for samples containing >20% missing data. Genomic relationship matrices (GRMs) were computed with missing data imputed as the mean genotype[32,33]. GRMs among the inbred pollen parents and seed parents were computed independently, and the hybrid GRM was then found as an average among the parental relationships.

In 2019 at MRS, an EM-38 MK2 surveyed Field N before 2019_NYH2 was planted. The georeferenced elevation (Alt) and electrical conductance (EC) data were interpolated over the entire field using ordinary Kriging[34]. To approximate soil curvature, first and second two-dimensional numerical derivatives were computed on the plot-level soil EC and Alt measurements, denoted as dEC, d2EC, dAlt, and d2Alt, respectively. Numerical derivatives were computed by averaging differences between nearby plots.

A MicaSense RedEdge 5-channel multi-spectral camera mounted onto an unoccupied aerial vehicle (UAV) captured images in the blue, green, red, near infrared, and red-edge spectra. At least 80% overlap along both image axes was ensured in the collected images. Flights were scheduled approximately once every week. Collected images were then processed into calibrated reflectance orthophotomosaics using Pix4dMapper software. The resulting reflectance orthophoto images were uploaded into ImageBreed, which enabled plot-polygon templates to be assigned to the field experiment design[35]. ImageBreed extracted NDVI into the database for each experimental plot and for each time point of image acquisition.

3. RESULTS

The first stage of the proposed approach used linear mixed models to partition NLEE from additive genetic effects using either random spatial or permanent environment (PE) effects. Spatial effects leverage information from the rows and columns of experimental plots in the field. Both two-dimensional spline (2DSpl) and separable autoregressive (AR1) models were considered, either independently across time or in multi-trait models, namely univariate and multivariate models (2DSplUni, AR1Uni, 2DSplMulti, AR1Multi), respectively[7,8]. As an example illustration in Figure 1, 2019_NYH2 2DSplUni NLEE were correlated with GY and soil data. 2DSplUni NLEE correlated up to 0.7 with GY 2DSpl at 110 days after planting (DAP) and correlated up to 0.5 and 0.3 with EC and d2Alt, respectively. In contrast to spatial effects, PE were computed using random regression models (RR). RR have computational benefits over multi-trait models and have been applied in maize[36,37]. Six RR PE covariance structures were tested: identity matrix (RRID), Euclidean distance matrix (RREuc), correlation matrix of AR1 spatial effects (RRAR1), correlation matrix of 2DSpl spatial effects (RR2DSpl), correlation of soil EC and derivatives (RRSoilEC), and correlation of soil Alt and derivatives (RRSoilAlt).

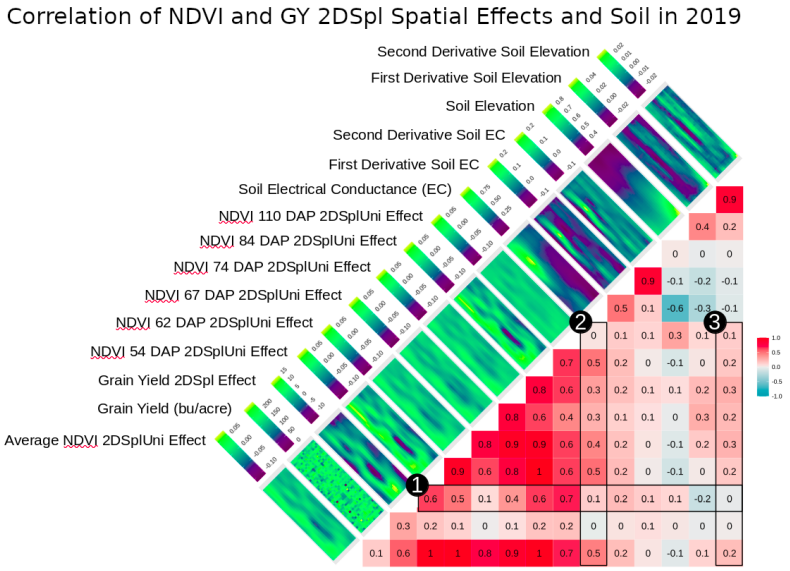

Figure 1. Representative plot of 2019_NYH2 2DSplUni NLEE over 6 time points correlated with GY and 2DSpl spatial effects of GY. Corresponding heatmaps show values over the rows and columns of all plots in the field. (1) Correlations of 0.1 to 0.7 between GY 2DSpl and 2DSplUni NLEE are found over the season with a high of 0.7 at 110 DAP. Soil EC, Alt, and the derivatives, are included with (2) correlations up to 0.5 for EC and (3) correlations up to 0.3 for d2Alt.

To compare the NLEE from the first stage to spatial effects affecting the agronomic traits, 2DSpl effects were computed independently for GY, EH, and GM, as illustrated in Figure 2. Within each of the 2017_NYH2, 2019_NYH2, and 2020_NYH2 field experiments, similar spatial trends emerged.

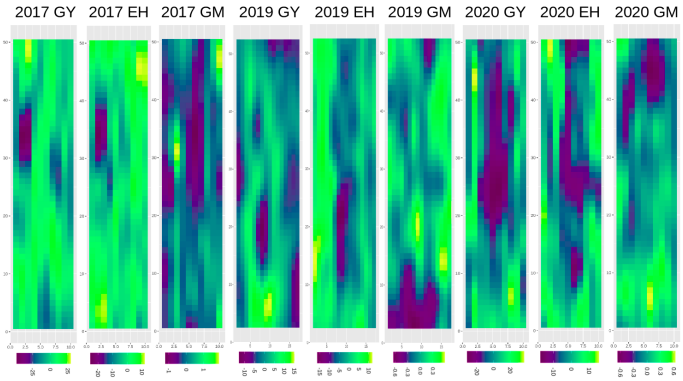

Figure 2. 2DSpl spatial random effects found independently in GY, GM, EH in the 2017_NYH2, 2019_NYH2, and 2020_NYH2 field experiments.

The second stage builds on GBLUP, $y = X\beta + Zu + e$ where $var(u) = \sigma_u^2 G$ and G is the GRM, using two distinct implementations: 1) defining L in $y = X\beta + Zu + Z_p u_p + e$ where $var(u_p) = \sigma_p^2 L$ or 2) setting FE as $y = X\beta + H\beta_H + Zu + e$. When using FE, two definitions were used: either an average of the NLEE were used (Havg) or the NLEE were divided into three groups of time points, representing the reproductive phases in terms of growing degree days (GDD) of early (0-1225 GDD), active (1226-1800 GDD), and late (1801-2500 GDD), and then averaged within each group (H3)[38]. Figure 3 illustrates genomic heritability, model fit, and genotypic effect estimation for GY, GM, and EH when defining L and FE, in (A) and (B), respectively. Baseline GBLUP and spatially corrected models of G, G+AR1, and G+2DSpl were compared to the best two-stage L models of G+L_AR1Uni,

G+L_2DSplUni, G+L_RRAR1, and G+L_RR2DSpl in (A), while the best two-stage FE models of G+Havg_AR1Uni, G+Havg_2DSplUni, G+H3_RRAR1, and G+H3_RR2DSpl are shown in (B). Significance (* < 0.05, + < 0.1) is compared with G using a t-test.

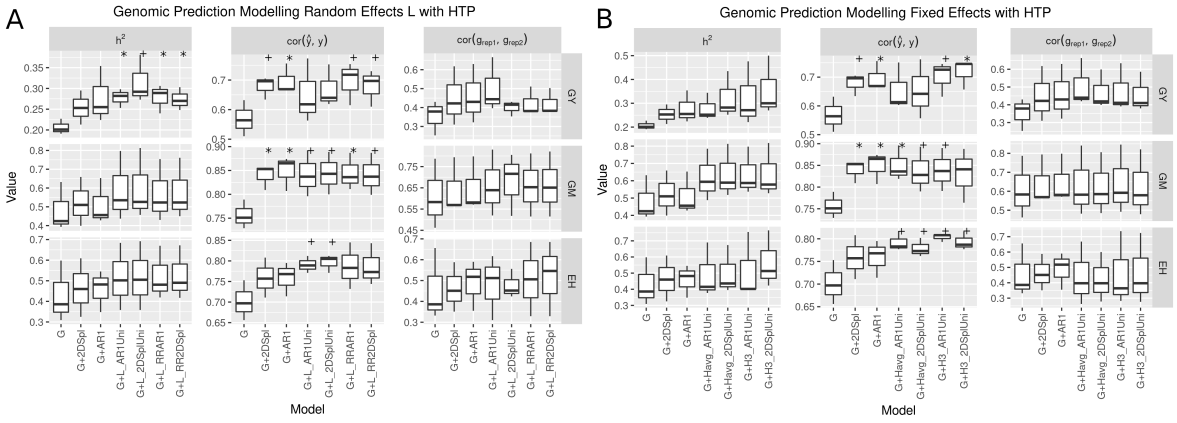

Figure 3. Genomic heritability (h^2), model fit (cor($\hat{y}$,y)), and genotypic effect estimation (cor(g_1,g_2)) for GY, GM, and EH, with NLEE implemented as L or as FE, in (A) and (B), respectively. The models G, G+2DSpl, and G+AR1 were baseline GBLUP and spatially corrected models, respectively. Models have L and FE defined using NLEE of corresponding name.

The second stage can use soil data rather than NLEE from the first stage. Figure 4 illustrates GP when defining L using empirical correlations (RRSoilEC, RRSoilAlt) and when defining FE as the soil values directly (Havg_SoilAlt, Havg_SoilEC, etc.). Model fit was improved, but may be overfitting.

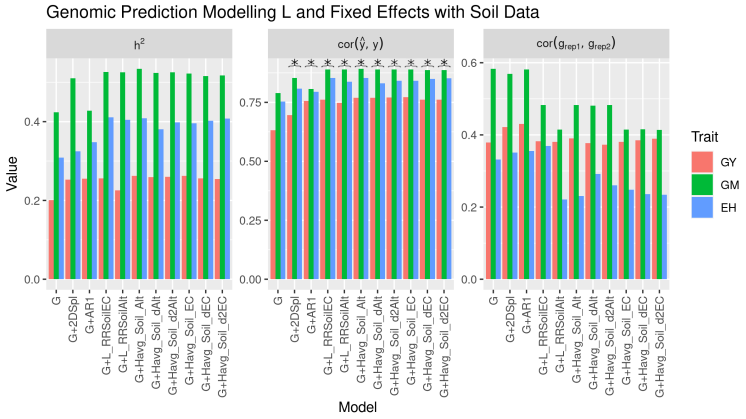

Figure 4. Genomic heritability (h^2), model fit (cor($\hat{y}$,y)), and genotypic effect estimation (cor(g_1,g_2)) for GY, GM, and EH, with NLEE implemented as L or as FE, using soil data.

4. Conclusion

The proposed two-stage approach significantly improves GP heritability and model fit for GY as well as model fit for GM and EH when compared to GBLUP; however, genotypic effect estimation across replicates is not significantly improved. Defining an empirical covariance (L) for random effects using NLEE from AR1Uni, 2DSplUni, RRAR1, and RR2DSpl models improves GP heritability for GY and model fit for GM most significantly. Defining H3 FE using AR1Uni NLEE improves GP model fit for all traits significantly. Soil EC, Alt, and the derivatives can significantly improve GP model fit by defining L or FE, but using NLEE improves GP more significantly. Soil EC and d2Alt are most correlated with 2DSplUni NLEE; however, defining L using RRAR1 and RR2DSpl NLEE increases GP heritability and model fit for GY and GM greater than 2DSplUni NLEE or any of the other tested models.

DATA AVAILABILITY STATEMENT

All field experimental data and genotyping data is made available by the G2F program through Cyverse. All aerial image data are available through https://imagebreed.org.

ACKNOWLEDGMENTS

This material is based upon work supported by the National Institute of Food and Agriculture, USDA, Hatch (100397, 1010428, 1013637, 1013641 M.A.G.) (1024080 K.R.R.), Iowa Corn and Cornell University startup funds (M.A.G. and K.R.R.), the Bill & Melinda Gates Foundation Nextgen Cassava grants (L.A.M.), and Foundation for Food and Agriculture CA20-SS-0000000103 (M.A.G. and K.R.R.).

REFERENCES

[1] Smith, A. B., Cullis, B. R. & Thompson, R. The analysis of crop cultivar breeding and evaluation trials: an overview of current mixed model approaches. *J. Agric. Sci.* **143**, 449–462 (2005).

[2] Van Es, H. M. & Van Es, C. L. Spatial nature of randomization and its effect on the outcome of field experiments. *Agron. J.* (1993).

[3] Brownie, C., Bowman, D. T. & Burton, J. W. Estimating Spatial Variation in Analysis of Data from Yield Trials: A Comparison of Methods. *Agronomy Journal* vol. 85 1244–1253 (1993).

[4] Xu, Y. Envirotyping for deciphering environmental impacts on crop plants. *Theor. Appl. Genet.* **129**, 653–673 (2016).

[5] Piepho, H. P., Möhring, J. & Williams, E. R. Why Randomize Agricultural Experiments? *Journal of Agronomy and Crop Science* vol. 199 374–383 (2013).

[6] Hoefler, R. *et al.* Do Spatial Designs Outperform Classic Experimental Designs? *Journal of Agricultural, Biological and Environmental Statistics* vol. 25 523–552 (2020).

[7] Gilmour, A. R., Cullis, B. R., Verbyla, A. P. & Verbyla, A. P. Accounting for Natural and Extraneous Variation in the Analysis of Field Experiments. *Journal of Agricultural, Biological, and Environmental Statistics* vol. 2 269 (1997).

[8] Rodríguez-Álvarez, M. X., Boer, M. P., van Eeuwijk, F. A. & Eilers, P. H. C. Correcting for spatial heterogeneity in plant breeding experiments with P-splines. *Spatial Statistics* vol. 23 52–71 (2018).

[9] Robbins, K. R., Backlund, J. E. & Schnelle, K. D. Spatial Corrections of Unreplicated Trials using a Two-dimensional Spline. *Crop Sci.* **52**, 1138–1144 (2012).

[10] White, J. W. *et al.* Field-based phenomics for plant genetics research. *Field Crops Research* vol. 133 101–112 (2012).

[11] Andrade-Sanchez, P. *et al.* Development and evaluation of a field-based high-throughput phenotyping platform. *Funct. Plant Biol.* **41**, 68–79 (2014).

[12] Sagan, V., Maimaitijiang, M., Sidike, P. & Eblimit, K. UAV-based high resolution thermal imaging for vegetation monitoring, and plant phenotyping using ICI 8640 P, FLIR Vue Pro R 640, and thermomap cameras. *Remote Sensing* (2019).

[13] Sun, D., Robbins, K., Morales, N., Shu, Q. & Cen, H. Advances in optical phenotyping of cereal crops. *Trends Plant Sci.* (2021) doi:10.1016/j.tplants.2021.07.015.

[14] Gitelson, A. A., Kaufman, Y. J., Stark, R. & Rundquist, D. Novel algorithms for remote estimation of vegetation fraction. *Remote Sens. Environ.* **80**, 76–87 (2002).

[15] Hunt, E. R. *et al.* A visible band index for remote sensing leaf chlorophyll content at the canopy scale. *Int. J. Appl. Earth Obs. Geoinf.* **21**, 103–112 (2013).

[16] Thorp, K. R., Thompson, A. L., Harders, S. J., French, A. N. & Ward, R. W. High-Throughput Phenotyping of Crop Water Use Efficiency via Multispectral Drone Imagery and a Daily Soil Water Balance Model. *Remote Sensing* **10**, 1682 (2018).

[17] Delegido, J., Verrelst, J., Alonso, L. & Moreno, J. Evaluation of Sentinel-2 red-edge bands for empirical estimation of green LAI and chlorophyll content. *Sensors* **11**, 7063–7081 (2011).

[18] Bannari, A., Shahid Khurshid, K., Staenz, K. & Schwarz, J. W. A Comparison of Hyperspectral Chlorophyll Indices for Wheat Crop Chlorophyll Content Estimation Using Laboratory Reflectance Measurements. *IEEE Transactions on Geoscience and Remote Sensing* vol. 45 3063–3074 (2007).
[19] Babar, M. A. *et al.* Spectral Reflectance to Estimate Genetic Variation for In-Season Biomass, Leaf Chlorophyll, and Canopy Temperature in Wheat. *Crop Science* vol. 46 1046–1057 (2006).
[20] Gage, J. L., Richards, E. & Lepak, N. In-Field Whole-Plant Maize Architecture Characterized by Subcanopy Rovers and Latent Space Phenotyping. *The Plant Phenome* (2019).
[21] Taghavi Namin, S., Esmaeilzadeh, M., Najafi, M., Brown, T. B. & Borevitz, J. O. Deep phenotyping: deep learning for temporal phenotype/genotype classification. *Plant Methods* **14**, 66 (2018).
[22] Wiesner-Hanks, T. *et al.* Millimeter-Level Plant Disease Detection From Aerial Photographs via Deep Learning and Crowdsourced Data. *Frontiers in Plant Science* vol. 10 (2019).
[23] Meuwissen, T. H. E., Hayes, B. J. & Goddard, M. E. Prediction of Total Genetic Value Using Genome-Wide Dense Marker Maps. *Genetics* vol. 157 1819–1829 (2001).
[24] Rutkoski, J. *et al.* Evaluation of Genomic Prediction Methods for Fusarium Head Blight Resistance in Wheat. *The Plant Genome* vol. 5 51–61 (2012).
[25] Daetwyler, H. D., Calus, M. P. L., Pong-Wong, R., de Los Campos, G. & Hickey, J. M. Genomic prediction in animals and plants: simulation of data, validation, reporting, and benchmarking. *Genetics* **193**, 347–365 (2013).
[26] Rutkoski, J. *et al.* Canopy Temperature and Vegetation Indices from High-Throughput Phenotyping Improve Accuracy of Pedigree and Genomic Selection for Grain Yield in Wheat. *G3* **6**, 2799–2808 (2016).
[27] Sakurai, K., Toda, Y., Kajiya-Kanegae, H. & Ohmori, Y. Time-series Multi-spectral Imaging in Soybean for Improving Biomass and Genomic Prediction Accuracy. *bioRxiv* (2021).
[28] Pérez-Valencia, D. M. *et al.* A two-stage approach for the spatio-temporal analysis of high-throughput phenotyping data. doi:10.1101/2021.08.10.455613.
[29] van Eeuwijk, F. A. *et al.* Modelling strategies for assessing and increasing the effectiveness of new phenotyping techniques in plant breeding. *Plant Sci.* **282**, 23–39 (2019).
[30] McFarland, B. A. *et al.* Maize genomes to fields (G2F): 2014–2017 field seasons: genotype, phenotype, climatic, soil, and inbred ear image datasets. *BMC Res. Notes* **13**, 71 (2020).
[31] Elshire, R. J. *et al.* A robust, simple genotyping-by-sequencing (GBS) approach for high diversity species. *PLoS One* **6**, e19379 (2011).
[32] Endelman, J. B. Ridge Regression and Other Kernels for Genomic Selection with R Package rrBLUP. *Plant Genome* **4**, 250–255 (2011).
[33] VanRaden, P. M. Efficient methods to compute genomic predictions. *J. Dairy Sci.* **91**, 4414–4423 (2008).
[34] Pebesma, E. J. Multivariable geostatistics in S: the gstat package. *Computers & Geosciences* vol. 30 683–691 (2004).
[35] Morales, N. *et al.* ImageBreed: Open-access plant breeding web–database for image-based phenotyping. *The Plant Phenome Journal* vol. 3 (2020).
[36] Anche, M. T. *et al.* Temporal covariance structure of multi-spectral phenotypes and their predictive ability for end-of-season traits in maize. *Theor. Appl. Genet.* **133**, 2853–2868 (2020).
[37] Schaeffer, L. R. Application of random regression models in animal breeding. *Livestock Production Science* vol. 86 35–45 (2004).
[38] Ahmad, L., Kanth, R. H., Parvaze, S. & Mahdi, S. S. Growing Degree Days to Forecast Crop Stages. *Experimental Agrometeorology: A Practical Manual* 95–98 (2017) doi:10.1007/978-3-319-69185-5_14.